Bone 127 (2019) 271–279

Contents lists available at ScienceDirect

Bone

journal homepage: www.elsevier.com/locate/bone

Full Length Article

A multi-imaging modality study of bone density, bone structure and the muscle - bone unit in end-stage renal disease☆

Mary B. Leonard[a,b,*], Felix W. Wehrli[c], Susan L. Ziolkowski[b], Erica Billig[d], Jin Long[b], Thomas L. Nickolas[e], Jeremy F. Magland[c], Snejana Nihtianova[f], Babette S. Zemel[g], Rita Herskovitz[g], Chamith S. Rajapakse[c,h]

[a] Department of Pediatrics, Stanford University School of Medicine, Stanford, CA, United States of America
[b] Department of Medicine, Stanford University School of Medicine, Stanford, CA, United States of America
[c] Department of Radiology, University of Pennsylvania, Philadelphia, PA, United States of America
[d] Department of Biostatistics and Epidemiology, University of Pennsylvania, Philadelphia, PA, United States of America
[e] Department of Medicine, Columbia University, New York, NY, United States of America
[f] Susanne M. Glasscock School of Continuing Studies, Rice University, Houston, TX, United States of America
[g] Department of Pediatrics, The Children's Hospital of Philadelphia, University of Pennsylvania, Philadelphia, PA, United States of America
[h] Department of Orthopaedic Surgery, University of Pennsylvania, Philadelphia, PA, United States of America

ARTICLE INFO

Keywords:
Chronic kidney disease
Sarcopenia
Bone mineral density
DXA
Quantitative computed tomography
MRI

ABSTRACT

End stage renal disease (ESRD) is associated with sarcopenia and skeletal fragility. The objectives of this cross-sectional study were to (1) characterize body composition, bone mineral density (BMD) and bone structure in hemodialysis patients compared with controls, (2) assess whether DXA areal BMD (aBMD) correlates with peripheral quantitative CT (pQCT) measures of volumetric BMD (vBMD), cortical dimensions and MRI measures of trabecular microarchitecture, and (3) determine the magnitude of bone deficits in ESRD after adjustment for muscle mass. Thirty ESRD participants, ages 25 to 64 years, were compared with 403 controls for DXA and pQCT outcomes and 104 controls for MRI outcomes; results were expressed as race- and sex- specific *Z*-scores relative to age. DXA appendicular lean mass index (ALMI kg/m^2) and total hip, femoral neck, ultradistal and 1/3rd radius aBMD were significantly lower in ESRD, vs. controls (all $p < 0.01$). pQCT trabecular vBMD ($p < 0.01$), cortical vBMD ($p < 0.001$) and cortical thickness (due to a greater endosteal circumference, $p < 0.02$) and MRI measures of trabecular number, trabecular thickness, and whole bone stiffness were lower (all $p < 0.01$) in ESRD, vs. controls. ALMI was positively associated with total hip, femoral neck, ultradistal radius and 1/3rd radius aBMD and with tibia cortical thickness ($R = 0.46$ to 0.64). Adjustment for ALMI significantly attenuated bone deficits at these sites: e.g. mean femoral neck aBMD was 0.79 SD lower in ESRD, compared with controls and this was attenuated to 0.33 with adjustment for ALMI. In multivariate models within the dialysis participants, pQCT trabecular vBMD and cortical area *Z*-scores were significant and independently (all $p < 0.02$) associated with DXA femoral neck, total hip, and ultradistal radius aBMD *Z*-scores. Cortical vBMD ($p = 0.01$) and cortical area ($p < 0.001$) Z-scores were significantly and independently associated with 1/3rd radius areal aBMD Z-scores ($R^2 = 0.62$). These data demonstrate that DXA aBMD captures deficits in trabecular and cortical vBMD and cortical area. The strong associations with ALMI, as an index of skeletal muscle, highlight the importance of considering the role of sarcopenia in skeletal fragility in patients with ESRD.

1. Introduction

CKD is associated with multiple risk factors for fracture, including abnormal vitamin D metabolism, secondary hyperparathyroidism, abnormal bone turnover, diabetes, malnutrition, inflammation, metabolic acidosis, and poor physical function [1–6]. Patients with chronic kidney disease (CKD) stages 3-5D (including dialysis patients) have markedly increased fracture rates, in association with greater

☆ Funding Sources: NIH K24-DK076808, R21-DK074105, R01-DK064966, R01-AR068382, R03-AR064577, K25-AR060283, T32-DK060455, UL1-RR024134 and UL1-TR000003.

* Corresponding author at: Stanford University Medical Center, 300 Pasteur Drive, Suite H310, Stanford, CA 94305, United States of America.
E-mail address: leonard5@stanford.edu (M.B. Leonard).

https://doi.org/10.1016/j.bone.2019.05.022
Received 4 April 2016; Received in revised form 16 May 2019; Accepted 16 May 2019
Available online 31 May 2019
8756-3282/ © 2019 Elsevier Inc. All rights reserved.

morbidity, mortality and cost, compared with the general population [3,7–14]. Furthermore, hip fracture incidence rates remain high despite purported improvements in the management of CKD mineral and bone disorder (CKD-MBD) and concurrent decreases in fracture rates in the general population [10,15–19].

The measurement of areal bone mineral density (aBMD) by DXA is the clinical standard to assess fracture risk in the general population. However, early publications addressing the relations between DXA aBMD and fracture risk in CKD were limited to cross-sectional studies in patients with and without prevalent fractures, yielding inconsistent results. Accordingly, the 2009 KDIGO Clinical Practice Guidelines for CKD-MBD recommended that aBMD testing *not* be performed routinely in patients with CKD stages 3-5D [20]. However, more recent prospective studies across the spectrum from CKD stage 3 to 5D demonstrated that DXA aBMD in the total hip, femoral neck, and ultradistal and 1/3rd radius predicted incident fractures [21–24]. In 2017, the Kidney Disease Improving Global Outcomes (KDIGO) leadership convened a Controversies Conference and concluded that DXA aBMD is reasonable to obtain if results may lead to additional interventions or medical management [25].

Multiple studies using conventional peripheral quantitative CT (pQCT) and high resolution pQCT (HR-pQCT) examined the structural underpinnings of skeletal fragility in CKD [26–29]. Overall, lower cortical area, thickness and volumetric BMD (vBMD), and abnormal trabecular microarchitecture were associated with prevalent fractures [27,28]. Although these studies provided important insights into fracture risk in CKD, none included healthy controls.

Numerous studies in the general population have documented strong correlations between bone and muscle mass in the context of exercise, disuse and aging [30–34]. The functional muscle–bone unit approach posits that bone adapts to the mechanical forces to which it is subjected in order to keep bone strength at a set point. Despite the fact that CKD is associated with sarcopenia [35] and impaired physical function, and poor physical function is a leading risk factor for fractures in CKD [36–38], no studies have examined associations among body composition and bone density and structure in adults with CKD.

This study will leverage the baseline DXA, pQCT and MRI data collected in 30 maintenance hemodialysis patients enrolled in a pilot and feasibility study of low magnitude mechanical stimuli [LMMS [39,40]] as an anabolic bone therapy. The study is strengthened by the inclusion of concurrent healthy reference participants for DXA, pQCT, and MRI outcomes. These unique reference data allow us to express the study outcomes as sex- and race-specific standard deviation scores (*Z*-scores) relative to age – facilitating the comparison of the magnitude of deficits across skeletal sites and imagining modalities without confounding by age, sex and race. The objectives of this study were to (1) characterize body composition and bone density, structure and microarchitecture in hemodialysis participants compared with reference participants, and (2) assess correlations among different imaging modalities in order to inform the interpretation of DXA results across sites, and (3) determine the impact of adjustment for muscle mass on differences in bone outcomes between hemodialysis participants and controls.

2. Methods

2.1. Study participants

Ambulatory maintenance hemodialysis patients, ages 21 to 65 years, treated at a single University of Pennsylvania (UPENN) dialysis facility, were eligible for a pilot and feasibility randomized clinical trial of daily exposure to 20 min of LMMS over a 6 month interval (Clinicaltrials.gov identifier NCT00364234). This analysis is limited to the baseline visit. Exclusion criteria included pregnancy, significant comorbidity (active malignancy or a history of myocardial infarction, congestive heart failure III-IV stage, cerebrovascular disease, liver failure, or neuropathy), a history of a fall within the prior 6 months, hip fracture or hip replacement, anticipated living-donor transplantation or relocation within the coming 6 months, and difficulty in ambulation, defined as difficulty climbing two flights of stairs or walking three blocks.

Healthy controls were enrolled in other studies using the same equipment and methods as the hemodialysis participants: (1) pQCT and DXA measurements were obtained in 502 adults, as previously described [41] and (2) MRI bone measurements were obtained in 104 adults. Exclusion criteria for the healthy controls included a history of chronic diseases or medications known to affect nutrition or bone health, such as a reported history of diabetes, malabsorption syndromes, CKD, liver disease, thyroid disease or malignancy. By design, the sex and race distributions of the healthy controls were pre-specified (approximately 50% male, and 50% black) for the purpose of generating sex- and race- specific reference data.

The protocols were approved by the Institutional Review Boards at the Children's Hospital of Philadelphia and UPENN. Informed consent was obtained from all participants.

2.2. Dialysis participant disease characteristics, medications and laboratory tests

The medical records were reviewed for the cause of underlying renal disease, date of onset of end stage renal disease (ESRD), medications and dialysis history. Renal disease was categorized as hypertension, diabetes, focal segmental glomerulosclerosis or other. Serum parathyroid hormone (PTH) levels were measured by Quest Diagnostic (Nichols Institute) using a chemiluminescence assay (sensitivity 3 pg/mL and with an interassay CV of 7%–9%).

2.3. Demographics and anthropometry

Weight and height were measured using a digital scale (Scaltronix, White Plains, NY) and stadiometer (Holtain Ltd., Crymych, UK), respectively. Participants self-identified their race according to the National Institute of Health categories.

2.4. DXA

DXA scans were performed using a Delphi/Discovery (Hologic, Bedford, MA, USA) densitometer. Whole body, posteroanterior (PA) lumbar spine (L1–L4), lateral lumbar spine (L2 − L3), left proximal femur and radius (ultradistal and 1/3rd) scans were obtained in the array mode using standard positioning techniques. Body composition measures indexed to height included whole body fat mass index (FMI, kg/m^2), lean body mass index (LBMI, kg/m^2), and appendicular lean mass index (ALMI, kg/m^2). The DXA instrument was calibrated using a hydroxyapatite spine phantom daily and a whole body phantom 3 times per week. The in vitro CV at our institution is < 1% for phantom scans and the in vivo CV is < 1% for spine BMD.

2.5. Peripheral QCT

Left tibia scans were obtained by pQCT (Stratec XCT2000 12-detector unit, Orthometrix) with a voxel size of 0.4 mm and slice thickness of 2.3 mm, and analyzed with Stratec software version 6.00, as previously described [41]. A scout view was obtained to place the reference line at the medial distal endplate. Bone measures were obtained at 3%, 38%, and 66% of tibia length proximal to the reference line. At the 3% metaphyseal site, scans were analyzed for trabecular vBMD (mg/cm^3). At the 38% diaphyseal site, scans were analyzed for cortical vBMD (mg/cm^3), cortical cross-sectional area (mm^2), cortical thickness (mm), periosteal circumference (mm), and endosteal circumference (mm). At the 66% site, scans were analyzed for calf muscle and fat cross-sectional area (mm^2). The pQCT measure of muscle density (mg/

Table 1
Participant demographics, BMI, and body composition in the hemodialysis participants and healthy controls.

	Hemodialysis		DXA and pQCT healthy controls*		ESRD vs. controls** *p*-value
	Black $N = 29$	Non-Black $N = 1$	Black $N = 178$	Non-Black $N = 235$	
Age, years	48.4 ± 10.3	48.8	44.6 ± 11.8	41.9 ± 13.5	
Male sex, n (%)	16 (56%)	1 (100%)	90 (51%)	105 (45%)	
Body mass index, kg/m^2					
Male	26.1 ± 4.4	22.3	27.0 ± 5.3	25.9 ± 4.4	0.55
Female	23.5 ± 4.8	–	29.9 ± 6.9	24.3 ± 4.8	< 0.01
Body composition *Z*-scores					
DXA whole body fat mass index (FMI)	−0.61 ± 0.90	−1.23	−0.26 ± 0.91	−0.60 ± 0.96	< 0.05
DXA whole body lean body mass index (LBMI)	−0.78 ± 1.03	−1.53	−0.22 ± 0.90	−0.26 ± 0.90	< 0.01
DXA appendicular lean mass index (ALMI)	−0.98 ± 1.04	−1.96	−0.25 ± 0.87	−0.23 ± 0.87	< 0.001
pQCT calf subcutaneous fat area	−0.63 ± 1.10	−0.15	0.03 ± 1.02	0.08 ± 1.00	< 0.01
pQCT calf muscle area	−1.00 ± 1.14	−1.93	−0.01 ± 0.99	0.01 ± 1.02	< 0.001
pQCT calf muscle density	−0.67 ± 0.90	0.18	−0.08 ± 1.10	0.00 ± 1.00	< 0.01

* Controls limited to those < 65 years of age, consistent with the ESRD enrollment criteria.
** *P* value limited to comparisons in black participants.

cm^3) was used as an index of intramuscular adipose tissue, as previously described [41,42]. Quality control was monitored daily using a hydroxyapatite phantom. The in vivo CV ranged from 0.5 to 1.6% for pQCT outcomes.

2.6. MRI acquisition and analysis

Distal tibia metaphysis of patients were scanned on a 1.5 Tesla whole-body MRI scanner (Siemens Sonata, Erlangen, Germany) using a surface coil and a fast large-angle spin echo (FLASE) pulse sequence [43]. Sequence parameters were: flip angle of 140°, TR/TE 80 ms/11.8 ms, 16.67-kHz bandwidth, and 137 × 137 × 410 μm^3 voxel size in 15 min 23 s. Tibia diaphysis was imaged at the 38% site using a commercial extremity coil and fast spin-echo sequence. Sequence parameters were: TR/TE = 5 s/16 ms, echo train length = 8, pixel size = 0.479 mm, slice thickness = 2 mm, and number of slices = 30.

The cortical and trabecular compartments were extracted for analysis by delineating the endosteal and periosteal boundaries using an operator guided segmentation program [44]. Integrity of the trabecular bone compartment was assessed at the distal tibia by calculating bone-volume fraction (BVF), trabecular spacing, trabecular number, and trabecular thickness using a Fuzzy Distance Transform Algorithm [45], and plate-to-rod ratio using local inertia anisotropy [46]. Whole cross-section axial stiffness at the distal tibia was computed using linear finite element analysis [47,48]. Cortical porosity was assessed at the tibial diaphysis as (1 − BV / TV) × 100% at each voxel averaged over the entire cortical bone region. The CVs were < 5% for MRI parameters [49].

3. Analysis plan

Statistical analyses were performed using Stata 13.0 (Stata Corp., College Station, TX). The bone and body composition outcomes varied substantially with age, sex and race, and were therefore converted to sex- and race-specific *Z*-scores relative to age in order to facilitate comparisons across demographic groups. First, the DXA body composition *Z*-scores were generated using National Health and Nutrition Examination Survey (NHANES) reference data in over 10,000 individuals [50]. The DXA aBMD and pQCT bone and body composition *Z*-scores were generated based on reference data in the 502 healthy controls. Cortical dimensions and calf muscle and fat area were highly correlated with tibia length (all $p < 0.001$); therefore, Z-scores for these outcomes were further adjusted for tibia length, as described [51]. The MRI bone structure Z-scores were generated based on the reference data in the 104 healthy controls.

Group differences between hemodialysis participants and controls were assessed using Student's *t*-tests, with adjustment for unequal variance, as needed, or with Wilcoxon rank-sum tests if not normally distributed. Because 29 of the 30 hemodialysis participants were black, these comparisons were limited to the black hemodialysis participants and black controls. PTH levels were natural log transformed and correlations with bone *Z*-scores were examined using Pearson correlations. Correlations among the DXA, pQCT and MRI bone *Z*-scores were assessed using Pearson or Spearman correlations, as indicated. Multivariate regression analyses were performed to identify pQCT and MRI *Z*-scores that were independently associated with DXA BMD Z-scores.

Correlations between ALMI and bone Z-scores were assessed using Pearson correlations. Subsequent regression models were generated to determine the impact of adjustment for ALMI Z-scores for those bone Z-scores that were associated with ALMI Z-scores and were lower in hemodialysis participants compared with controls.

Although multiple comparisons were performed across numerous correlated bone measures, a Bonferroni correction is not appropriate since it assumes that these measures are independent. Therefore, we interpreted isolated findings with caution and examined the consistency of the overall results.

4. Results

4.1. Participant characteristics

The participant demographic characteristics are summarized in Table 1. All but one hemodialysis participants was black; therefore, the data are presented stratified on race. Among black participants, body mass index (BMI) was significantly lower in women with ESRD compared with controls.

Among the hemodialysis participants, the underlying cause of CKD was hypertension in 12, diabetes in 2, FSGS in 6, other in 5 and unknown in 5. The median [interquartile range (IQR)] duration of ESRD was 4.9 (1.4 to 11.1) years. At enrollment, 28 participants were treated with phosphate binders: 18 were prescribed a single binder (8 calcium-containing, 9 sevelamer, and 1 lanthanum) and 10 were prescribed both a calcium-containing binder and either sevelamer or lanthanum. All but two participants were treated with an active vitamin D sterol (3 calcitriol and 25 paricalcitol) and 10 were prescribed cinacalcet. The median (IQR) PTH level was 290 (184, 440) pg/mL.

4.2. Body composition

Table 1 summarizes the body composition *Z*-scores in the hemodialysis participants and healthy controls. The mean DXA body

Table 2
DXA, pQCT, and MRI bone outcomes in hemodialysis participants and healthy controls.

	Hemodialysis		DXA and pQCT controls		MRI controls		Dialysis vs. controls**
	Black N = 29	Non-Black *N* = 1	Black *N* = 178	Non-Black N = 235	Black *N* = 53	Non-Black *N* = 51	p-Value
DXA BMD *Z*-scores							
PA spine BMD	−0.35 ± 1.35	−0.68	0.00 ± 1.00	−0.01 ± 1.02			0.20
Lateral spine BMD	−0.17 ± 1.57	1.00	−0.01 ± 1.03	0.01 ± 0.98			0.61
Total hip BMD	−0.81 ± 1.52	−0.74	−0.01 ± 0.99	0.02 ± 1.01			< 0.01
Femoral neck BMD	−0.81 ± 1.45	−1.20	0.00 ± 1.01	0.02 ± 1.01			< 0.01
1/3rd radius BMD	−0.93 ± 1.16	−0.74	0.01 ± 0.99	0.00 ± 0.99			< 0.001
Ultradistal radius BMD	−1.13 ± 1.23	−1.31	0.01 ± 1.01	0.01 ± 0.98			< 0.001
pQCT *Z*-scores							
Trabecular BMD	−0.92 ± 1.45	0.09	−0.03 ± 1.01	0.01 ± 1.00			< 0.01
Cortical BMD	−1.21 ± 1.13	−0.69	−0.02 ± 1.00	−0.01 ± 1.00			< 0.001
Cortical area	−0.19 ± 1.26	0.20	0.03 ± 0.92	0.00 ± 0.96			0.26
Cortical thickness	−0.45 ± 1.22	0.74	−0.07 ± 0.99	0.01 ± 0.99			< 0.05
Periosteal circumference	0.29 ± 1.02	−0.36	0.11 ± 0.85	−0.01 ± 0.89			0.33
Endosteal circumference	0.58 ± 1.08	−0.73	0.11 ± 0.97	0.06 ± 0.89			< 0.02
Micro-MRI Z-score							
Trabecular bone volume fraction	−1.53 ± 1.49	0.24			0.00 ± 0.99	0.00 ± 0.99	< 0.001
Trabecular thickness	−0.71 ± 2.36	0.16			0.00 ± 0.99	0.00 ± 0.99	< 0.01
Median (IQR)	−1.40 (−2.07, 0.14)						
Trabecular number	−1.58 ± 1.01	0.25			0.00 ± 0.99	0.00 ± 0.99	< 0.001
Trabecular spacing	1.94 ± 1.51	−0.31			0.00 ± 0.99	0.00 ± 0.99	< 0.001
Median (IQR)	1.89 (0.97, 2.79)						
Plates to rod	−0.27 ± 1.15	−0.36			0.00 ± 0.99	0.00 ± 0.99	0.15
Median (IQR)	−0.24 (−1.22, 0.04)						
Cortical porosity	0.75 ± 0.91	−0.13			0.00 ± 0.99	0.00 ± 0.99	< 0.01
Median (IQR)	0.75 (0.27, 1.06)						
Stiffness	−1.98 ± 1.08	−1.67			0.00 ± 0.99	0.00 ± 0.99	< 0.001

Data presented as mean ± SD, and as median (interquartile range) if skewed.
** p value limited to comparisons in black participants.

composition Z-scores in our local healthy controls were less than zero, consistent with the fact that their mean BMI was lower than the mean in the NHANES participants [52] who were the source of the DXA body composition reference data; this may be due to our exclusion criteria for healthy controls (e.g. no diabetes). The mean ± SD pQCT muscle and fat *Z*-scores were approximately 0.0 ± 1.0 in the healthy controls, as expected, given that these individuals were the reference data source for these outcomes.

ESRD was associated with significantly lower FMI, LBMI, ALMI, calf muscle area, calf fat area, and muscle density *Z*-scores, compared with healthy controls. The lower muscle density is consistent with greater intramuscular adipose tissue [53].

4.3. Bone density, structure and microarchitecture

Table 2 and Fig. 1 summarizes the DXA, pQCT and MRI bone results. ESRD was associated with lower DXA total hip, femoral neck, 1/3rd radius and ultradistal radius aBMD *Z*-scores, and lower pQCT trabecular and cortical vBMD and cortical thickness *Z*-scores. The lower cortical thickness was due to endocortical thinning with significantly greater endosteal circumference *Z*-scores, compared with controls. The MRI results further characterized the trabecular deficits with a markedly lower bone volume fraction, trabecular thickness, trabecular number and whole bone stiffness, compared with controls. The plate-to-rod ratio was not different than controls. Cortical porosity was greater, compared with controls. PTH levels were not associated with any of the bone outcome *Z*-scores.

Table 3 summarizes the univariate correlations among the bone Z-scores within the hemodialysis participants, with shading indicating significant correlations. It is noteworthy that the total hip and femoral neck (mixed cortical and trabecular bone) *Z*-scores were significantly associated with pQCT measures of trabecular vBMD and cortical structure, while the 1/3rd radius (an almost entirely cortical site) was significantly associated with pQCT measures of cortical vBMD and cortical structure. The MRI measure of tibia trabecular bone volume fraction and whole bone stiffness were associated with pQCT trabecular vBMD.

Additional multivariate models within the dialysis participants demonstrated that trabecular vBMD and cortical area *Z*-scores were significant and independently (all $p < 0.02$) associated with femoral neck ($R^2 = 0.42$), total hip ($R^2 = 0.48$), and ultradistal radius ($R^2 = 0.63$) aBMD Z-scores. Cortical vBMD ($p = 0.01$) and cortical area ($p < 0.001$) *Z*-scores were significantly and independently associated with 1/3rd radius aBMD *Z*-scores ($R^2 = 0.62$).

4.4. Correlations among muscle and bone outcomes

Table 4 demonstrates that ALMI *Z*-scores were significantly and positively correlated ($R = 0.46$ to 0.64) with *Z*-scores for aBMD in the total hip, femoral neck, ultradistal radius, and 1/3rd radius by DXA, and cortical structure in the tibia by pQCT in the individuals with ESRD. Table 5 summarizes the results of multivariable models used to determine the impact of adjustment for ALMI *Z*-scores on the bone outcomes that were lower in ESRD, compared with controls, and were associated with ALMI Z-score. Adjustment for the lower ALMI Z-scores in the ESRD participants attenuated the group differences. For example, the mean femoral neck aBMD Z-score was 0.79 lower in ESRD, compared with controls and this difference was attenuated to 0.33 with adjustment for the lower ALMI Z-scores in the ESRD patients. Cortical thickness was only marginally lower in ESRD compared with controls and this difference was no longer significant after adjustment for ALMI Z-scores.

5. Discussion

This study demonstrated significant sarcopenia and reductions in

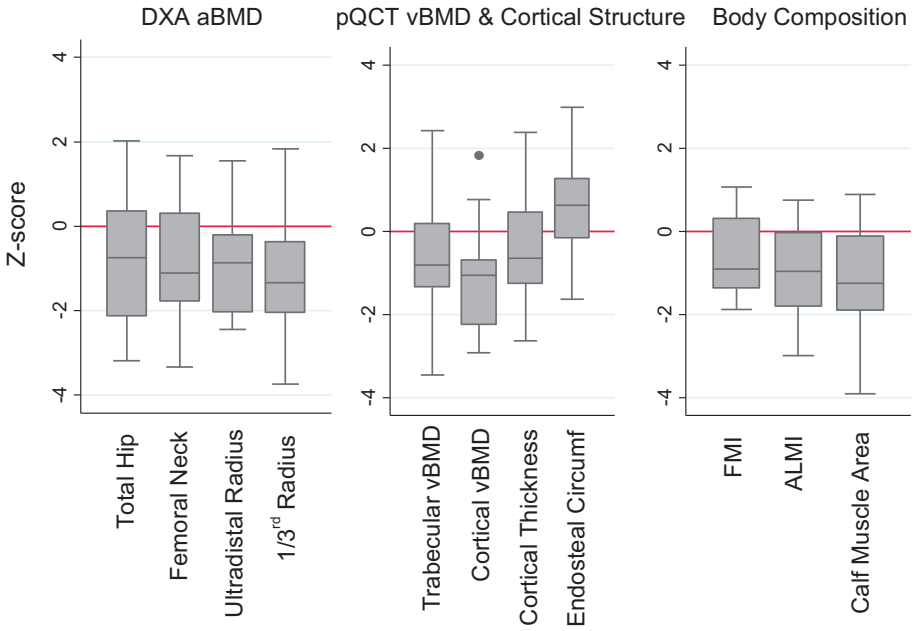

Fig. 1. Bone and body composition Z-scores in hemodialysis participants.
(FMI: fat mass index; ALMI: appendicular lean mass index.)

tibia trabecular and cortical vBMD and cortical thickness (due to endocortical bone loss) in adults on maintenance hemodialysis, compared with healthy controls. The MRI analyses revealed that the lower trabecular vBMD was due to reductions in both trabecular number and thickness, resulting in decreased stiffness. DXA aBMD was significantly lower in the radius and proximal femur but not in the spine in the ESRD participants. ALMI was highly correlated with cortical structure, and adjustment for the muscle deficits attenuated the deficits in the total hip BMD, femoral neck BMD, ultradistal radius BMD, 1/3rd radius BMD, and tibia diaphysis cortical area in the ESRD participants. The lower muscle density is consistent with increased intramuscular adipose tissue, suggesting poor muscle quality as well as low muscle mass [54]. This study is strengthened by the inclusion of a large number of controls. The use of standard deviation scores provided insights into the magnitude of musculoskeletal deficits across anatomical sites and across imaging modalities.

Early cross-sectional studies suggested that DXA did not discriminate between CKD patients with and without fractures. This was attributed to the fact that the metabolic abnormalities that accompany CKD may have opposing effects on trabecular and cortical bone mass; DXA is a two dimension projection technique that does not distinguish between superimposed trabecular and cortical bone [55]. While it is well-established that secondary hyperparathyroidism in CKD is associated with *decreases* in cortical vBMD and loss of endocortical bone [56–60], reports that elevated PTH levels preserved or *increased* trabecular bone were based on studies in patients with primary hyperparathyroidism [61,62]. A recent study in 33 adults on dialysis and 33 controls reported that ESRD was associated with decreased trabecular number and abnormal trabecular microarchitecture, similar to our results. Therefore, the fact that ESRD is associated with decreases in both trabecular and cortical bone mass may explain the fact that recent longitudinal studies showed that DXA aBMD predicted fractures in CKD stages 3 to 5D and in transplant recipients [21–23,63].

In these recent studies, proximal femur (total hip and/or femoral neck) aBMD consistently predicted fractures [21–23]. However, the two studies that included spine aBMD reported no association [22] or a weak association [21] with incident fractures. ESRD patients may develop endplate osteosclerosis (“rugger jersey spine”) and aortic calcification which falsely elevate aBMD. This may explain the poor ability of spine aBMD to predict fracture in prior studies and the lack of differences in spine aBMD *Z*-scores between our ESRD and control participants. In the study that compared the ability of DXA sites to predict an incident fracture, the ultradistal radius was the site with the greatest area under the curve (0.74, 95% CI 0.65 to 0.83). A cross-sectional study also identified the ultradistal site as the DXA site with greatest ability to discriminate between CKD patients with and without prevalent fractures [28].

Although prior studies have compared QCT and DXA in the spine and total hip in dialysis patients [64–66], this is the first study to correlate DXA aBMD results with trabecular vBMD, cortical vBMD and cortical structure. The use of Z-scores eliminated the confounding effects of age, sex, and race in these comparisons. The multivariate models demonstrated that a substantial proportion of the variability in the DXA measures of aBMD in the total hip, femoral neck and ultradistal radius were explained by tibia trabecular vBMD and cortical area, but not cortical vBMD. In contrast, the DXA aBMD in the 1/3rd radius (a cortical site) reflected both cortical vBMD and area; these two cortical measures explained 63% of the variability in DXA aBMD despite differences in skeletal site. This supports the 2013 International Society of Clinical Densitometry recommendations that forearm DXA is the preferred site in patients with hyperparathyroidism [67].

To our knowledge, this is the first study to explore the relations of muscle mass with bone density and structure in adults with ESRD. The pattern of correlations summarized in Table 4 indicates that the underlying association is between ALMI and cortical structure. The potential mechanisms for this association are two-fold. First, biomechanical forces generated by muscle stimulate the addition of new bone onto bone surfaces experiencing high strains [68]. This is predominantly mediated by suppression of osteocyte production of sclerostin, an inhibitor of bone formation that increases in states of unloading [69]. For example, Armamento-Villareal, et al., reported that obese adults randomized to progressive resistance training exhibited significant increases in thigh muscle volume and total hip aBMD. Greater gains in muscle volume were significantly associated with greater decreases in sclerostin concentrations [33]. In multiple stepwise regression analyses, changes in thigh muscle volume were an independent predictor of change in total hip BMD. Studies of athletes, e.g. baseball pitchers and racquet sport players, consistently demonstrated

Table 3
Correlations among bone outcomes within the hemodialysis participants.

	R (p value)	DXA areal BMD Z-scores				pQCT volumetric BMD and cortical structure Z-scores						MicroMRI trabecular architecture Z-scores		
		Lat spine BMD	Total hip BMD	Fem neck BMD	1/3rd radius BMD	Ultradistal radius BMD	Trab vBMD	Cortical vBMD	Cortical area	Peri Circ	Endo Circ	BVF	Cortical porosity	Stiffness
DXA	PA spine BMD	**0.73 (< 0.001)**	**0.80 (< 0.001)**	**0.71 (< 0.001)**	**0.55 (0.002)**	**0.63 (< 0.001)**	**0.46 (0.02)**	0.20 (0.30)	0.41 (0.03)	0.20 (0.30)	−0.23 (0.23)	−0.19 (0.35)	0.10 (0.59)	−0.21 (0.30)
	Lateral spine BMD		**0.67 (< 0.001)**	**0.68 (< 0.001)**	0.24 (0.21)	**0.38 (0.04)**	**0.48 (0.01)**	0.07 (0.71)	0.15 (0.43)	0.06 (0.76)	−0.07 (0.74)	−0.22 (0.26)	0.17 (0.39)	−0.12 (0.54)
	Total hip BMD			**0.91 (< 0.001)**	**0.62 (< 0.001)**	**0.70 (< 0.001)**	0.59 (0.001)	0.19 (0.32)	0.53 (< 0.01)	0.13 (0.49)	**−0.44 (0.02)**	0.02 (0.90)	0.08 (0.70)	0.00 (0.98)
	Femoral neck BMD				**0.46 (0.01)**	**0.64 (< 0.001)**	**0.56 (< 0.01)**	−0.05 (0.80)	**0.44 (0.02)**	0.22 (0.226)	−0.22 (0.25)	0.12 (0.57)	0.17 (0.38)	0.10 (0.63)
	1/3rd radius BMD					**0.79 (< 0.001)**	0.33 (0.09)	**0.56 (0.001)**	**0.72 (< 0.001)**	0.31 (0.09)	**−0.44 (0.01)**	0.30 (0.12)	−0.30 (0.11)	0.18 (0.35)
	UltradistalRadius BMD						**0.65 (< 0.001)**	**0.47 (< 0.01)**	**0.63 (< 0.001)**	**0.39 (0.03)**	−0.26 (0.17)	**0.47 (0.01)**	−0.15 (0.43)	**0.41 (0.03)**
pQCT	Trab vBMD							0.28 (0.15)	0.26 (0.18)	0.04 (0.83)	−0.23 (0.24)	**0.47 (0.01)**	−0.09 (0.67)	0.52 (< 0.01)
	Cortical vBMD								**0.38 (0.04)**	0.03 (0.88)	**−0.40 (0.03)**	0.19 (0.33)	**−0.42 (0.02)**	0.13 (0.50)
	Cortical area									**0.67 (< 0.001)**	−0.27 (0.15)	0.34 (0.08)	−0.30 (0.11)	0.15 (0.45)
	Peri Circ										**0.50 (< 0.01)**	0.31 (0.11)	−0.06 (0.74)	0.16 (0.43)
	Endo Circ											0.03 (0.86)	0.24 (0.20)	0.05 (0.81)
Micro-MRI	BVF												−0.12 (0.20)	**0.75 (< 0.001)**
	Cortical porosity													−0.17 (0.08)

The bold indicates those correlations that were statistically significant, defined as $p < 0.05$.

Table 4
Correlations among appendicular lean mass index and bone outcomes within the hemodialysis participants.

R (p value)	DXA areal BMD *Z*-scores						pQCT volumetric BMD and Cortical Structure Z-scores						Micro-MRI Bone ZZ-scores		
	PA Spine BMD	Lat Spine BMD	Total Hip BMD	Fem Neck BMD	1/3rd Radius BMD	UD Radius BMD	Trab vBMD	Cortical vBMD	Cortical Area	Cortical Thick	Peri Circ	Endo Circ	BVF	Cortical Porosity	Stiffness
Appendicular lean mass index *Z*-score	0.39 (0.06)	0.37 (0.08)	**0.48 (0.02)**	**0.46 (0.03)**	**0.57 (< 0.01)**	**0.57 (< 0.01)**	−0.03 (0.91)	0.19 (0.37)	**0.64 (< 0.001)**	**0.53 (< 0.01)**	**0.57 (< 0.01)**	−0.56 (0.78)	0.10 (0.65)	−0.03 (0.87)	0.12 (0.61)

Correlations are presented as R (p-value).
The bold indicates those correlations that were statistically significant, defined as $p < 0.05$.

Table 5
Impact of adjustment of bone outcomes for appendicular lean mass index.

	ESRD vs. control		ESRD vs. control, adjusted for appendicular lean mass index *Z*-score	
	β (95% CI)	p	β (95% CI)	p
Total hip BMD *Z*-score	−0.79 (−1.22, −0.35)	< 0.001	−0.33 (−0.72, 0.06)	0.10
Femoral neck BMD Z-score	−0.84 (−1.27, −0.41)	< 0.001	−0.43 (−0.82, −0.03)	0.03
1/3rd radius BMD Z-score	−0.98 (−1.39, −0.56)	< 0.001	−0.79 (−1.20, −0.37)	< 0.001
Ultradistal radius BMD Z-score	−1.15 (−1.57, −0.74)	< 0.001	−0.81 (−1.20, −0.41)	< 0.001
Cortical thickness Z-score	−0.39 (−0.80, 0.03)	0.04	−0.03 (−0.43, 0.36)	0.91

greater cortical thickness and area in the loaded, compared with unloaded arm [70]. Therefore, the patterns we observed in our study are consistent with the effects of biomechanical loading. Second, the association may not be causal in nature, rather reflecting the adverse effect of ESRD on both bone and muscle metabolism through alternations in sex steroids, growth hormone, and insulin-like growth factors. However, a recent small randomized controlled trial of intradialytic cycling exercise demonstrated a beneficial effect on DXA aBMD in the femoral neck (and not the lumbar spine) [71]. These data highlight the need for further studies of the effects of exercise and muscle mass on bone density, structure and strength in dialysis patients.

The cross-sectional design, small sample size, and limited measures of mineral metabolism are the primary limitations of this study. The pattern of cortical bone deficits was consistent with secondary hyperparathyroidism; however, PTH levels were not associated with any bone outcomes. This is likely due to the fact that the PTH levels were only available at the time of the study, while the imaging results reflected the cumulative effects of CKD-MBD. Prior longitudinal studies did document that higher PTH levels were associated with rapid cortical bone loss in children [58,72], and adults [60] with CKD. Vitamin D concentrations were not available. The strong association of ALMI with cortical structure and aBMD may not be causal in nature; rather ESRD is associated with many threats to both bone and muscle metabolism. Physical activity interventions are needed to determine if gains in muscle mass and strength are associated with increases in bone density and structure in dialysis patients. Additional limitations include the lack of measures of physical activity and tests of physical function; however, lack of these data does not hamper the comparison of imaging results. Finally, 29 of 30 ESRD participants were black. In the absence of CKD, it is well established that black individuals have higher BMD compared with white individuals [73–75]. For this reason, all of our study results are expressed as race-specific *Z*-scores. Studies in dialysis patients also demonstrated higher BMD of the spine and total hip in black compared to white individuals [64,76]. It is not known if the impact of ESRD on bone density and structure varies according to race; therefore, the bone deficits observed in the ESRD participants here may not be generalizable.

The study is uniquely strengthened by the large number of control participants and the use of standard deviation scores. This represents an important advance compared with reports of percent differences in bone outcomes between CKD participants and controls because different components of bone strength normally demonstrate different degrees of variability. For example, among our young adult pQCT controls, 1 SD was 12% of the mean for trabecular vBMD, but only 2% of the mean for cortical vBMD. Therefore, cortical vBMD varies to a smaller degree and small percentage reductions in cortical vBMD represent substantial group differences. When vBMD is expressed as mg/cm^3 (as opposed to *Z*-scores) in this study, trabecular and cortical vBMD were, on average, 14% and 3% lower in the ESRD participants, compared with controls, respectively, adjusted for age, sex and race (data not shown). These seemingly large difference in the magnitude of bone deficits at trabecular versus cortical sites are a function of differences in normal variability, as the Z-scores were approximately −1 for both outcomes.

In summary, these data suggest that DXA aBMD measures in the proximal femur and radius capture CKD effects on trabecular and cortical vBMD and cortical structure. The strong associations with ALMI, as an index of skeletal muscle, highlight the importance of considering the role of sarcopenia in the skeletal fragility in patients with CKD. Longitudinal studies are needed to establish correlations among changes in these bone measures, to examine associations with falls and fractures, and to determine the impact of pharmacologic or exercise interventions.

Declaration of Competing Interest

All authors state that they have no conflicts of interest.

References

[1] C. Delgado, S. Shieh, B. Grimes, G.M. Chertow, L.S. Dalrymple, G.A. Kaysen, J. Kornak, K.L. Johansen, Association of self-reported frailty with falls and fractures among patients new to dialysis, Am. J. Nephrol. 42 (2015) 134–140.
[2] Y. Maruyama, M. Taniguchi, J.J. Kazama, K. Yokoyama, T. Hosoya, T. Yokoo, T. Shigematsu, K. Iseki, Y. Tsubakihara, A higher serum alkaline phosphatase is associated with the incidence of hip fracture and mortality among patients receiving hemodialysis in Japan, Nephrol. Dial. Transplant. 29 (2014) 1532–1538.
[3] M. Maravic, A. Ostertag, P.U. Torres, M. Cohen-Solal, Incidence and risk factors for hip fractures in dialysis patients, Osteoporos. Int. 25 (2014) 159–165.
[4] M.K. Ma, D.Y. Yap, T.P. Yip, S.L. Lui, W.K. Lo, Charlson co-morbidity index and albumin significantly associated with fracture risk in peritoneal dialysis patients, Nephrology (Carlton) 18 (2013) 365–368.
[5] V. Panuccio, G. Enia, R. Tripepi, R. Aliotta, F. Mallamaci, G. Tripepi, C. Zoccali, Pro-

inflammatory cytokines and bone fractures in CKD patients. An exploratory single centre study, BMC Nephrol. 13 (2012) 134.
[6] A. Kato, R. Kido, Y. Onishi, N. Kurita, M. Fukagawa, T. Akizawa, S. Fukuhara, Association of serum bicarbonate with bone fractures in hemodialysis patients: the mineral and bone disorder outcomes study for Japanese CKD stage 5D patients (MBD-5D), Nephron Clin Pract 128 (2014) 79–87.
[7] T.L. Nickolas, D.J. McMahon, E. Shane, Relationship between moderate to severe kidney disease and hip fracture in the United States, J. Am. Soc. Nephrol. 17 (2006) 3223–3232.
[8] A.M. Ball, D.L. Gillen, D. Sherrard, N.S. Weiss, S.S. Emerson, S.L. Seliger, B.R. Kestenbaum, C. Stehman-Breen, Risk of hip fracture among dialysis and renal transplant recipients, Jama 288 (2002) 3014–3018.
[9] A.M. Alem, D.J. Sherrard, D.L. Gillen, N.S. Weiss, S.A. Beresford, S.R. Heckbert, C. Wong, C. Stehman-Breen, Increased risk of hip fracture among patients with end-stage renal disease, Kidney Int. 58 (2000) 396–399.
[10] Z.Z. Lin, J.J. Wang, C.R. Chung, P.C. Huang, B.A. Su, K.C. Cheng, C.C. Chio, C.C. Chien, Epidemiology and mortality of hip fracture among patients on dialysis: Taiwan National Cohort Study, Bone 64 (2014) 235–239.
[11] A. Mittalhenkle, D.L. Gillen, C.O. Stehman-Breen, Increased risk of mortality associated with hip fracture in the dialysis population, Am. J. Kidney Dis. 44 (2004) 672–679.
[12] F. Tentori, K. McCullough, R.D. Kilpatrick, B.D. Bradbury, B.M. Robinson, P.G. Kerr, R.L. Pisoni, High rates of death and hospitalization follow bone fracture among hemodialysis patients, Kidney Int. 85 (2014) 166–173.
[13] K.E. Ensrud, L.Y. Lui, B.C. Taylor, A. Ishani, M.G. Shlipak, K.L. Stone, J.A. Cauley, S.A. Jamal, D.M. Antoniucci, S.R. Cummings, Osteoporotic Fractures Research G, Renal function and risk of hip and vertebral fractures in older women, Arch. Intern. Med. 167 (2007) 133–139.
[14] V. Sathiyakumar, R. Thakore, S.E. Greenberg, A.C. Dodd, W. Obremskey, M.K. Sethi, Risk factors for discharge to rehabilitation among hip fracture patients, Am J Orthop (Belle Mead NJ) 44 (2015) E438–E443.
[15] A.T. Mathew, A. Hazzan, K.D. Jhaveri, G.A. Block, S. Chidella, L. Rosen, J. Wagner, S. Fishbane, Increasing hip fractures in patients receiving hemodialysis and peritoneal dialysis, Am. J. Nephrol. 40 (2014) 451–457.
[16] A.C. Beaubrun, R.D. Kilpatrick, J.K. Freburger, B.D. Bradbury, L. Wang, M.A. Brookhart, Temporal trends in fracture rates and postdischarge outcomes among hemodialysis patients, J. Am. Soc. Nephrol. 24 (2013) 1461–1469.
[17] S.S. Nair, A.A. Mitani, B.A. Goldstein, G.M. Chertow, D.W. Lowenberg, W.C. Winkelmayer, Temporal trends in the incidence, treatment, and outcomes of hip fracture in older patients initiating dialysis in the United States, Clin. J. Am. Soc. Nephrol. 8 (2013) 1336–1342.
[18] T.J. Arneson, S. Li, J. Liu, R.D. Kilpatrick, B.B. Newsome, W.L. St Peter, Trends in hip fracture rates in US hemodialysis patients, 1993-2010, Am. J. Kidney Dis. 62 (2013) 747–754.
[19] S.M. Kim, S. Liu, J. Long, M.E. Montez-Rath, M.B. Leonard, G.M. Chertow, Declining rates of hip fracture in end-stage renal disease: analysis from the 2003-2011 Nationwide inpatient sample, J. Bone Miner. Res. 32 (2017) 2297–2303.
[20] KDIGO clinical practice guideline for the diagnosis, evaluation, prevention, and treatment of Chronic Kidney Disease-Mineral and Bone Disorder (CKD-MBD), Kidney Int. (2009) S1–130 Suppl.
[21] S.L. West, C.E. Lok, L. Langsetmo, A.M. Cheung, E. Szabo, D. Pearce, M. Fusaro, R. Wald, J. Weinstein, S.A. Jamal, Bone mineral density predicts fractures in chronic kidney disease, J. Bone Miner. Res. 30 (2015) 913–919.
[22] S. Iimori, Y. Mori, W. Akita, T. Kuyama, S. Takada, T. Asai, M. Kuwahara, S. Sasaki, Y. Tsukamoto, Diagnostic usefulness of bone mineral density and biochemical markers of bone turnover in predicting fracture in CKD stage 5D patients–a single-center cohort study, Nephrol. Dial. Transplant. 27 (2012) 345–351.
[23] R.H. Yenchek, J.H. Ix, M.G. Shlipak, D.C. Bauer, N.J. Rianon, S.B. Kritchevsky, T.B. Harris, A.B. Newman, J.A. Cauley, L.F. Fried, Health A, Body Composition S, Bone mineral density and fracture risk in older individuals with CKD, Clin. J. Am. Soc. Nephrol. 7 (2012) 1130–1136.
[24] K.L. Naylor, A.X. Garg, G. Zou, L. Langsetmo, W.D. Leslie, L.A. Fraser, J.D. Adachi, S. Morin, D. Goltzman, B. Lentle, S.A. Jackson, R.G. Josse, S.A. Jamal, Comparison of fracture risk prediction among individuals with reduced and normal kidney function, Clin. J. Am. Soc. Nephrol. 10 (2015) 646–653.
[25] M. Ketteler, G.A. Block, P. Evenepoel, M. Fukagawa, C.A. Herzog, L. McCann, S.M. Moe, R. Shroff, M.A. Tonelli, N.D. Toussaint, M.G. Vervloet, M.B. Leonard, Executive summary of the 2017 KDIGO chronic kidney disease-mineral and bone disorder (CKD-MBD) guideline update: what's changed and why it matters, Kidney Int. 92 (2017) 26–36.
[26] S.A. Jamal, J. Gilbert, C. Gordon, D.C. Bauer, Cortical pQCT measures are associated with fractures in dialysis patients, J. Bone Miner. Res. 21 (2006) 543–548.
[27] T.L. Nickolas, S. Cremers, A. Zhang, V. Thomas, E. Stein, A. Cohen, R. Chauncey, L. Nikkel, M.T. Yin, X.S. Liu, S. Boutroy, R.B. Staron, M.B. Leonard, D.J. McMahon, E. Dworakowski, E. Shane, Discriminants of prevalent fractures in chronic kidney disease, J. Am. Soc. Nephrol. 22 (2011) 1560–1572.
[28] T.L. Nickolas, E. Stein, A. Cohen, V. Thomas, R.B. Staron, D.J. McMahon, M.B. Leonard, E. Shane, Bone mass and microarchitecture in CKD patients with fracture, J. Am. Soc. Nephrol. 21 (2010) 1371–1380.
[29] S. Jamal, A.M. Cheung, S. West, C. Lok, Bone mineral density by DXA and HR pQCT can discriminate fracture status in men and women with stages 3 to 5 chronic kidney disease, Osteoporos. Int. 23 (2012) 2805–2813.
[30] N.K. Lebrasseur, S.J. Achenbach, L.J. Melton 3rd, S. Amin, S. Khosla, Skeletal muscle mass is associated with bone geometry and microstructure and serum insulin-like growth factor binding protein-2 levels in adult women and men, J. Bone Miner. Res. 27 (2012) 2159–2169.
[31] L.J. Melton 3rd, B.L. Riggs, S.J. Achenbach, S. Amin, J.J. Camp, P.A. Rouleau, R.A. Robb, A.L. Oberg, S. Khosla, Does reduced skeletal loading account for age-related bone loss? J. Bone Miner. Res. 21 (2006) 1847–1855.
[32] A.K. Wong, P.M. Cawthon, K.W. Peters, S.R. Cummings, C.L. Gordon, Y. Sheu, K. Ensrud, M. Petit, J.M. Zmuda, E. Orwoll, J. Cauley, Bone-muscle indices as risk factors for fractures in men: the osteoporotic fractures in men (MrOS) study, J. Musculoskelet. Neuronal Interact. 14 (2014) 246–254.
[33] R. Armamento-Villareal, L. Aguirre, N. Napoli, K. Shah, T. Hilton, D.R. Sinacore, C. Qualls, D.T. Villareal, Changes in thigh muscle volume predict bone mineral density response to lifestyle therapy in frail, obese older adults, Osteoporos. Int. 25 (2014) 551–558.
[34] M.Y. Pang, M.C. Ashe, J.J. Eng, Muscle weakness, spasticity and disuse contribute to demineralization and geometric changes in the radius following chronic stroke, Osteoporos. Int. 18 (2007) 1243–1252.
[35] S.L. Ziolkowski, J. Baker, J. Simard, G. Chertow, M.B. Leonard, Sarcopenia, relative sarcopenia and excess adiposity in chronic kidney disease, Journal of Cachexia, Sarcopenia and Muscle- Clinical Reports 3 (2018) 1–11.
[36] K.L. Johansen, L.S. Dalrymple, C. Delgado, G.A. Kaysen, J. Kornak, B. Grimes, G.M. Chertow, Association between body composition and frailty among prevalent hemodialysis patients: a US renal data system special study, J. Am. Soc. Nephrol. 25 (2014) 381–389.
[37] S.A. Jamal, R.E. Leiter, V. Jassal, C.J. Hamilton, D.C. Bauer, Impaired muscle strength is associated with fractures in hemodialysis patients, Osteoporos. Int. 17 (2006) 1390–1397.
[38] S.L. West, S.A. Jamal, C.E. Lok, Tests of neuromuscular function are associated with fractures in patients with chronic kidney disease, Nephrol. Dial. Transplant. 27 (2012) 2384–2388.
[39] D.P. Kiel, M.T. Hannan, B.A. Barton, M.L. Bouxsein, E. Sisson, T. Lang, B. Allaire, D. Dewkett, D. Carroll, J. Magaziner, E. Shane, E.T. Leary, S. Zimmerman, C.T. Rubin, Low-magnitude mechanical stimulation to improve bone density in persons of advanced age: a randomized, placebo-controlled trial, J. Bone Miner. Res. 30 (2015) 1319–1328.
[40] L. Slatkovska, S.M. Alibhai, J. Beyene, H. Hu, A. Demaras, A.M. Cheung, Effect of 12 months of whole-body vibration therapy on bone density and structure in post-menopausal women: a randomized trial, Ann. Intern. Med. 155 (2011) 668–679 (w205).
[41] J.F. Baker, M. Davis, R. Alexander, B.S. Zemel, S. Mostoufi-Moab, J. Shults, M. Sulik, D.J. Schiferl, M.B. Leonard, Associations between body composition and bone density and structure in men and women across the adult age spectrum, Bone 53 (2013) 34–41.
[42] J.F. Baker, J. Von Feldt, S. Mostoufi-Moab, G. Noaiseh, E. Taratuta, W. Kim, M.B. Leonard, Deficits in muscle mass, muscle density, and modified associations with fat in rheumatoid arthritis, Arthritis Care Res (Hoboken) 66 (2014) 1612–1618.
[43] J.F. Magland, M.J. Wald, F.W. Wehrli, Spin-echo micro-MRI of trabecular bone using improved 3D fast large-angle spin-echo (FLASE), Magn. Reson. Med. 61 (2009) 1114–1121.
[44] C.S. Rajapakse, M.B. Leonard, Y.A. Bhagat, W. Sun, J.F. Magland, F.W. Wehrli, Micro-MR imaging-based computational biomechanics demonstrates reduction in cortical and trabecular bone strength after renal transplantation, Radiology 262 (2012) 912–920.
[45] P.K. Saha, F.W. Wehrli, Measurement of trabecular bone thickness in the limited resolution regime of in vivo MRI by fuzzy distance transform, IEEE Trans. Med. Imaging 23 (2004) 53–62.
[46] B. Vasilic, C.S. Rajapakse, F.W. Wehrli, Classification of trabeculae into three-dimensional rodlike and platelike structures via local inertial anisotropy, Med. Phys. 36 (2009) 3280–3291.
[47] C.S. Rajapakse, J.F. Magland, M.J. Wald, X.S. Liu, X.H. Zhang, X.E. Guo, F.W. Wehrli, Computational biomechanics of the distal tibia from high-resolution MR and micro-CT images, Bone 47 (2010) 556–563.
[48] J.F. Magland, N. Zhang, C.S. Rajapakse, F.W. Wehrli, Computationally-optimized bone mechanical modeling from high-resolution structural images, PLoS One 7 (2012) e35525.
[49] S.C. Lam, M.J. Wald, C.S. Rajapakse, Y. Liu, P.K. Saha, F.W. Wehrli, Performance of the MRI-based virtual bone biopsy in the distal radius: serial reproducibility and reliability of structural and mechanical parameters in women representative of osteoporosis study populations, Bone 49 (2011) 895–903.
[50] T.L. Kelly, K.E. Wilson, S.B. Heymsfield, Dual energy X-ray absorptiometry body composition reference values from NHANES, PLoS One 4 (2009) e7038.
[51] V. Lo Re 3rd, K. Lynn, E.R. Stumm, J. Long, M.S. Nezamzadeh, J.F. Baker, A.N. Hoofnagle, A.J. Kapalko, K. Mounzer, B.S. Zemel, P. Tebas, J.R. Kostman, M.B. Leonard, Structural bone deficits in HIV/HCV-Coinfected, HCV-Monoinfected, and HIV-Monoinfected women, J. Infect. Dis. 212 (2015) 924–933.
[52] C.L. Ogden, M.D. Carroll, B.K. Kit, K.M. Flegal, Prevalence of childhood and adult obesity in the United States, 2011-2012, Jama 311 (2014) 806–814.
[53] B.H. Goodpaster, D.E. Kelley, F.L. Thaete, J. He, R. Ross, Skeletal muscle attenuation determined by computed tomography is associated with skeletal muscle lipid content, J Appl Physiol (1985) 89 (2000) 104–110.
[54] B. Cheema, H. Abas, B. Smith, A.J. O'Sullivan, M. Chan, A. Patwardhan, J. Kelly, A. Gillin, G. Pang, B. Lloyd, K. Berger, B.T. Baune, M.F. Singh, Investigation of skeletal muscle quantity and quality in end-stage renal disease, Nephrology (Carlton) 15 (2010) 454–463.
[55] T.L. Nickolas, M.B. Leonard, E. Shane, Chronic kidney disease and bone fracture: a growing concern, Kidney Int. 74 (2008) 721–731.
[56] A.M. Parfitt, A structural approach to renal bone disease, J. Bone Miner. Res. 13 (1998) 1213–1220.

[57] T.A. Hopper, F.W. Wehrli, P.K. Saha, J.B. Andre, A.C. Wright, C.P. Sanchez, M.B. Leonard, Quantitative microcomputed tomography assessment of intratrabecular, intertrabecular, and cortical bone architecture in a rat model of severe renal osteodystrophy, J. Comput. Assist. Tomogr. 31 (2007) 320–328.
[58] R.J. Wetzsteon, H.J. Kalkwarf, J. Shults, B.S. Zemel, B.J. Foster, L. Griffin, C.F. Strife, D.L. Foerster, D.K. Jean-Pierre, M.B. Leonard, Volumetric bone mineral density and bone structure in childhood chronic kidney disease, J. Bone Miner. Res. 26 (2011) 2235–2244.
[59] H.C. Schober, Z.H. Han, A.J. Foldes, M.S. Shih, D.S. Rao, R. Balena, A.M. Parfitt, Mineralized bone loss at different sites in dialysis patients: implications for prevention, J. Am. Soc. Nephrol. 9 (1998) 1225–1233.
[60] T.L. Nickolas, E.M. Stein, E. Dworakowski, K.K. Nishiyama, M. Komandah-Kosseh, C.A. Zhang, D.J. McMahon, X.S. Liu, S. Boutroy, S. Cremers, E. Shane, Rapid cortical bone loss in patients with chronic kidney disease, J. Bone Miner. Res. 28 (2013) 1811–1820.
[61] D.W. Dempster, R. Muller, H. Zhou, T. Kohler, E. Shane, M. Parisien, S.J. Silverberg, J.P. Bilezikian, Preserved three-dimensional cancellous bone structure in mild primary hyperparathyroidism, Bone 41 (2007) 19–24.
[62] M. Parisien, S.J. Silverberg, E. Shane, L. de la Cruz, R. Lindsay, J.P. Bilezikian, D.W. Dempster, The histomorphometry of bone in primary hyperparathyroidism: preservation of cancellous bone structure, J. Clin. Endocrinol. Metab. 70 (1990) 930–938.
[63] S. Akaberi, O. Simonsen, B. Lindergard, G. Nyberg, Can DXA predict fractures in renal transplant patients? Am. J. Transplant. 8 (2008) 2647–2651.
[64] H.H. Malluche, D.L. Davenport, T. Cantor, M.C. Monier-Faugere, Bone mineral density and serum biochemical predictors of bone loss in patients with CKD on dialysis, Clin. J. Am. Soc. Nephrol. 9 (2014) 1254–1262.
[65] U. Barnas, A. Schmidt, G. Seidl, A. Kaider, P. Pietschmann, G. Mayer, A comparison of quantitative computed tomography and dual X-ray absorptiometry for evaluation of bone mineral density in patients on chronic hemodialysis, Am. J. Kidney Dis. 37 (2001) 1247–1252.
[66] G.A. Blomquist, D.L. Davenport, H.W. Mawad, M.C. Monier-Faugere, H.H. Malluche, Diagnosis of low bone mass in CKD-5D patients, Clin. Nephrol. 85 (2016) 77–83.
[67] J.T. Schousboe, J.A. Shepherd, J.P. Bilezikian, S. Baim, Executive summary of the 2013 International Society for Clinical Densitometry Position Development Conference on bone densitometry, J. Clin. Densitom. 16 (2013) 455–466.
[68] C.H. Turner, S.J. Warden, T. Bellido, L.I. Plotkin, N. Kumar, I. Jasiuk, J. Danzig, A.G. Robling, Mechanobiology of the skeleton, Sci. Signal. 2 (2009) pt3.
[69] A.G. Robling, P.J. Niziolek, L.A. Baldridge, K.W. Condon, M.R. Allen, I. Alam, S.M. Mantila, J. Gluhak-Heinrich, T.M. Bellido, S.E. Harris, C.H. Turner, Mechanical stimulation of bone in vivo reduces osteocyte expression of Sost/sclerostin, J. Biol. Chem. 283 (2008) 5866–5875.
[70] S.J. Warden, J. Carballido-Gamio, K.G. Avin, M.E. Kersh, R.K. Fuchs, R. Krug, R.J. Bice, Adaptation of the proximal humerus to physical activity: a within-subject controlled study in baseball players, Bone 121 (2019) 107–115.
[71] M.T. Liao, W.C. Liu, F.H. Lin, C.F. Huang, S.Y. Chen, C.C. Liu, S.H. Lin, K.C. Lu, C.C. Wu, Intradialytic aerobic cycling exercise alleviates inflammation and improves endothelial progenitor cell count and bone density in hemodialysis patients, Medicine (Baltimore) 95 (2016) e4134.
[72] M.R. Denburg, A.K. Tsampalieros, I.H. de Boer, J. Shults, H.J. Kalkwarf, B.S. Zemel, D. Foerster, D. Stokes, M.B. Leonard, Mineral metabolism and cortical volumetric bone mineral density in childhood chronic kidney disease, J. Clin. Endocrinol. Metab. 98 (2013) 1930–1938.
[73] B.S. Zemel, H.J. Kalkwarf, V. Gilsanz, J.M. Lappe, S. Oberfield, J.A. Shepherd, M.M. Frederick, X. Huang, M. Lu, S. Mahboubi, T. Hangartner, K.K. Winer, Revised reference curves for bone mineral content and areal bone mineral density according to age and sex for black and non-black children: results of the bone mineral density in childhood study, J. Clin. Endocrinol. Metab. 96 (2011) 3160–3169.
[74] M.B. Leonard, A. Elmi, S. Mostoufi-Moab, J. Shults, J.M. Burnham, M. Thayu, L. Kibe, R.J. Wetzsteon, B.S. Zemel, Effects of sex, race, and puberty on cortical bone and the functional muscle bone unit in children, adolescents, and young adults, J. Clin. Endocrinol. Metab. 95 (2010) 1681–1689.
[75] A.C. Looker, L.G. Borrud, J.P. Hughes, B. Fan, J.A. Shepherd, M. Sherman, Total body bone area, bone mineral content, and bone mineral density for individuals aged 8 years and over: United States, 1999-2006, Vital Health Stat. 11 (2013) 1–78.
[76] C.O. Stehman-Breen, D. Sherrard, A. Walker, R. Sadler, A. Alem, J. Lindberg, Racial differences in bone mineral density and bone loss among end-stage renal disease patients, Am. J. Kidney Dis. 33 (1999) 941–946.